**To cite this document:** GUILLON, Damien ; RIVALLANT, Samuel ; BARRAU
Experimental and numerical study of the splaying mode crush of CFRP laminates. In: *ICCM 17 - 17th International Conference on Composite Materials*, 27-31 July 2009, Edinburgh, UK.

# EXPERIMENTAL AND NUMERICAL STUDY OF THE SPLAYING MODE CRUSH OF CFRP LAMINATES

D. Guillon[1], S. Rivallant[2], JJ. Barrau[3], C. Petiot[4], P. Thevenet[4], B.Malherbe[5]
[1] CETIM ; 74 route de la Jonnelière, 44326 NANTES
[2] Université de Toulouse /ISAE/DMSM ; 10 av. E. Belin, 31055 Toulouse, France
[3] Université de Toulouse/UPS/LGMT ; 118 Rte de Narbonne, 31062 Toulouse, France
[4] EADS IW/SP/ME ; 12 rue Pasteur, 92152 Suresnes, France
[5] Airbus France/EDSAZ ; 316 route de Bayonne, 31060 Toulouse, France
samuel.rivallant@isae.fr

## SUMMARY

Thanks to an innovative plate crushing test fixture, elementary crushing modes of CFRP laminates have been observed and analysed for static and dynamic loading. These analyses enabled to propose a 2D explicit finite element model at mesoscale for the simulation of splaying mode, with a good correlation between model and test data.

*Keywords: laminate, crushing, energy absorption, experimental/numerical correlation*

## INTRODUCTION

Thanks to their high strength-to-weight ratio, composite materials are widely used in the field of transport and especially in aerospace applications, where weight savings are important. But specificity and complexity of composite fractures modes make difficult the prediction of the mechanical behaviour of composite structures subjected to crush loading.

Numerous studies [1,2] have been done in the last decades and the interest in crashworthiness is still present as show the recent works on the subject [3]. But there is still a lake in numerical simulation. Most of the models developed in the last few years [4,5] are based on global tests characterisation that make the model depend on global parameters, which do not permit to have predictive models. Some models [6,7] are based on material characteristics, but often need an a priori knowledge of the crush damage mode developed in the crush front. The challenge today in crashworthiness simulation is then to be able, from elementary material characterisation data, to predict both crush damage modes and energy absorption in any structures.

In this study, a model for splaying mode of crushing plates is presented. Simulation is based only on elementary material mechanical characteristics. Experimental tests made with an innovative plate crush test fixture enable to have precise data (load, displacement, global behaviour) for experiment/simulation correlation.

## EXPERIMENTAL ACHIEVEMENT

This paragraph presents the test fixture and a summary of main results of the experimental study made on composite laminated plates subjected to crush loading. More experimental results can be found in [8].

### Test fixture

The test fixture (figure 1) has been designed to improve plate crushing fixtures found in literature. It is made of four vertical adjustable guides which avoid buckling of the specimen, and two horizontal adjustable guides. These ones are localised just beneath the vertical guides so that a gap exists between horizontal guides and the metallic base plate where the laminate crashes. Such a concept has been developed at the same time by Feraboli [3]. This avoid tearing of the plate observed in most of the plate crushing fixtures [9,10], and ensure that the boundary conditions are the same along the whole width of the plate, just above the crushing front. Two main uprights carry the guides without interference with the crush front. Visualisation holes have been made to let the crush front visible.

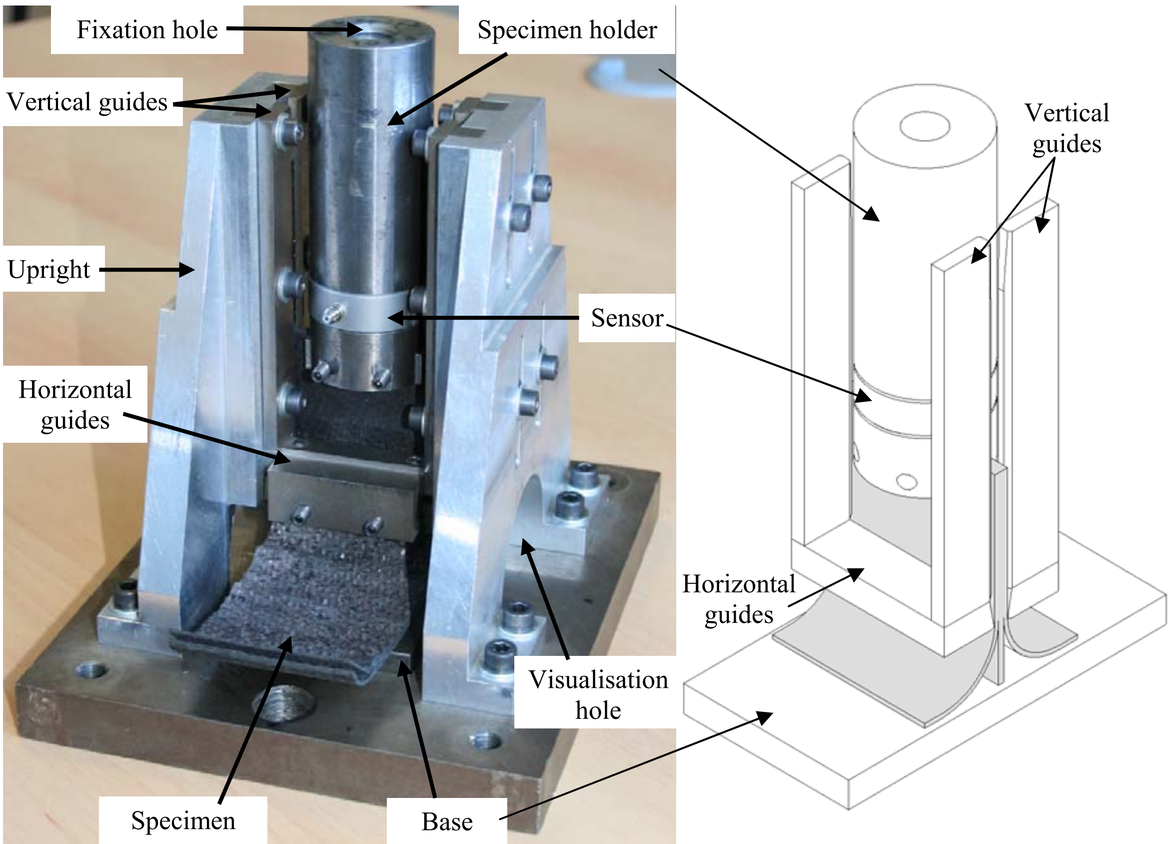


Figure 1: Test fixture: photo and simplified drawing (without uprights)

The thickness of the specimen can vary from 0 to 10mm. The gap (unsupported height between the base plate and the horizontal guides) can vary from 0 to 40 mm.

The laminate is fixed to a steel cylinder which is the interface with the static machine or the drop tower (dynamic tests). During crushing, plate and cylinder go down between the uprights and the vertical guides. At the bottom of the cylinder, a 120 kN Kistler piezoelectric sensor measures the crushing load. The small distance between the specimen and the sensor limits the mechanical filtering of the signal, allowing high precision in the dynamic crush load measurement. A high speed camera is used to have a real-time observation of the crushing front on the side of the plate. The filming speed is 20000 fps, with a 512x256 pixels resolution.

### Specimen

Specimens are 160x60mm flat laminated plates. White graduations are drawn on the edge of the specimen each 5 mm. Each test is defined by three parameters:

- Trigger mechanism: three different triggers, shown in figure 2,

- Crush speed: 20 mm/min for static test, and 5 m/s impact speed for drop tower tests,

- Laminate configuration: three materials were tested: 1) Vicotex 914/42%/G803 carbon-epoxy prepreg fabrics with stacking sequences $[(0°/90°),(+45°/-45°)]_{4/s}$ and $[(0°/90°)]_{8/s}$, 2) Hexply M21/35/268/T700GC thick unidirectional carbon-epoxy prepreg with stacking sequences $[0°,45°,-45°,0°,90°]_{2/s}$ and $[45°,0°,-45°,90°]_{4/s}$, 3) Hexply M21/35/134/T700GC thin unidirectional carbon-epoxy prepreg with stacking sequences $[45°,-45°]_{8/s}$ and $[0°,90°]_{8/s.}$

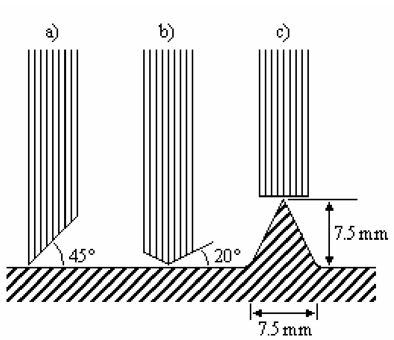


Figure 2: Trigger: a) chamfer - b) steeple - c)metallic blade

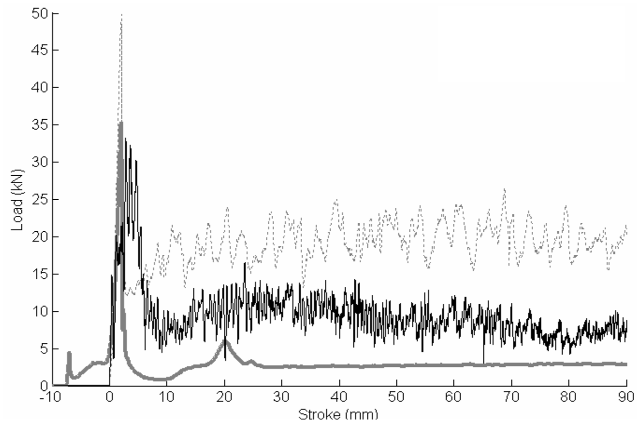


Figure 3: Load-Displacement curves
top: fractured splaying (G803/914, static)
middle: mixed mode (T700/M21, dynamic)
bottom: undamaged splaying (G803/914, static)

### Experimental results

The numerous experiments made enabled to observe the different crush modes of composite laminated plates (figure 4). Crush mechanisms are homogeneous through the width of the plate, thus the real-time pictures of the side of the crushed laminate allow observation and understanding of crush modes. Following is shortly described some of the main modes observed.

Undamaged splaying occurs when the laminate is flexible enough to bend without localized damages in plies during the crush. Small ratio between interface toughness and ply strength favour this crush mode. Energy absorbed is low: less than 10 kJ/kg, (see figure 3). Fractured splaying occurs when the laminate suffers repetitive localized damages in plies due to bending during the crush. An obstacle, like a debris wedge, in the front separating two splaying arms is necessary to maintain this mode. Fragmentation occurs when plies reach the metallic base at right angle and can not slip on the base. Failure appears continuously at microscopic scale. Energy absorbed is much higher: up to 50 kJ/kg, depending on the number of damaged plies (see figure 3). But fragmentation is not a stable crush mode, plies crush evolving from fragmentation to bending, leading to undamaged or fractured splaying crush mode.

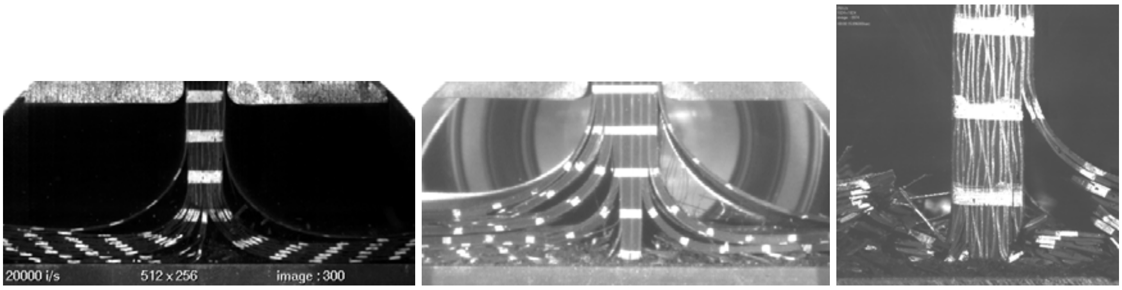


Figure 4: Examples of crush modes observed (from left to right) :
undamaged splaying mode: laminate of G803/914 - Chamfer trigger
Mixed mode: laminate of T700/M21 - chamfer trigger
Fragmentation: laminate of G803/914- chamfer trigger

## NUMERICAL SIMULATION

The numerical simulation is based on a dynamic test. The specimen is a laminated plate made of twenty 0,25 mm thick UD T700/M21 plies, with the stacking sequence $[0°,45°,-45°,0°,90°]_{2/S}$. The trigger is a metallic blade. The crush mode obtained for this test configuration is a splaying mode with multi-delamination of the plies. The initial speed of the falling mass is 5 m/s. Load/time curve, load/displacement curve and high speed videos of the tests are available to make precise correlation between test and simulation. The calculation is made with Abaqus explicit code.

### Model description

In this model, x is the crushing direction and z the direction perpendicular to the plate (see figure 5). Directions 1, 2 and 3 represent fibre direction, transverse direction and through the thickness direction of the ply. 0° corresponds to the crushing direction (x).

The laminated plate is modelled in three-dimension (figure 5). Only 100 mm length of the plate is modelled, to reduce calculation time, which is long enough to have realistic boundary conditions on the metallic plate and the guides. Each layer is modelled with one square thick shell elements in the ply thickness (continuum shell in Abaqus). Dimensions of elements are 0.23 mm in the thickness, and 0,25 mm in the two other directions. The shell element mid-plan corresponds to the ply mid-plan (plan xy). Layers are separated by 3D cohesive elements. The thickness of the interface is 0.02 mm, close to the tenth of the ply thickness. Details of plate mesh and plate stacking sequence are given in fig 6.

To reduce calculation time, only one element is used in the width of the plate (y direction). The model is then made of 8000 thick shell elements and 7600 cohesive elements, which give around 100000 degrees of freedom.

The metallic blade is defined as a rigid boundary condition with contact (penalty method) and friction (friction coefficient of 0.1). The guides are represented by two rigid half-planes, with similar contact and friction rules.

Additional masses are added at the top of the plate, to represent the mass of the falling weight used in the test. An initial speed of 5 m/s is applied to the plate and these additional masses.

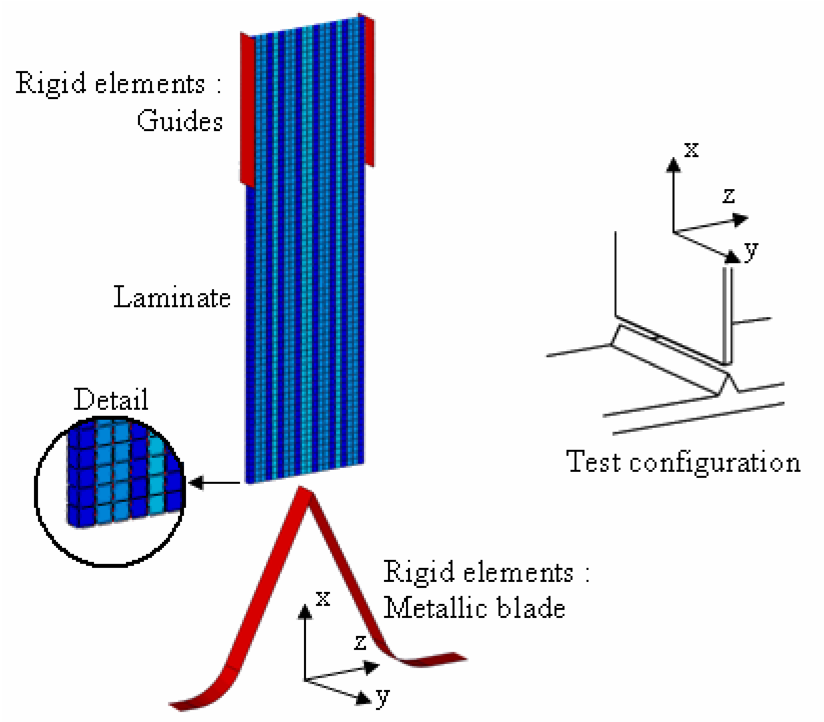


Figure 5: Finite element model

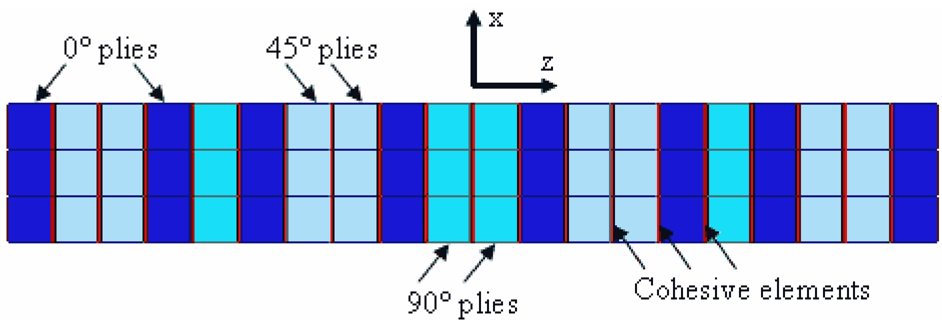


Figure 6: Mesh details

**Damage in ply**

The pseudo 2D characteristic of the model leads to define different materials for 0° and 90° plies in one hand, and 45° plies in the other hand.

For 0° and 90° plies, the behaviour is linear elastic damageable. Damage initiation is given by Hashin criteria, reduced to plane stresses. The mechanical characteristics are given in table 1, where $X^T$, $X^C$, $Y^T$, $Y^C$ and $S_C$ are the tensile and compressive strength in fibre direction, the tensile and compressive strength in the transverse direction, and the in-plane shear strength. Then, for each of the four damage mode, a damage variable is defined: dft, dfc, dmt, dmc for fibre rupture mode in tension and compression, and matrix rupture mode in tension and compression. The element rigidity decrease linearly with the strain, which give the following evolution of damage variables:

$$d_i = \frac{\varepsilon_i^f \cdot \left(\varepsilon_i - \varepsilon_i^0\right)}{\varepsilon_i \cdot \left(\varepsilon_i^f - \varepsilon_i^0\right)} \qquad (1)$$

Where $\varepsilon_i$ is the strain concerned by the damage mode i, $\varepsilon_i^0$ is the strain when Hashin criterion is reached for the damage mode i, and $\varepsilon_i^f$ is the strain when total rupture is reached in mode i.

The rupture strain $\varepsilon_i^f$ is calculated so that the surface energy dissipated in the element is equal to the energy dissipated in an elementary stable compression/tensile crack test propagation (fibre in compression: $G_{FC}$, fibre in tension: $G_{FT}$). The values used in fibre direction are extrapolated from tests made by Pinho [11], on T300/913. The values for matrix rupture are extrapolated from interlaminar fracture mechanics test. See table 1 for the values.

The material degradation law, taking into account a few couplings is given below:

$$[\sigma] = \frac{1}{\alpha}\begin{bmatrix} (1-d_f)E_1 & (1-d_f)(1-d_m)\nu_{21}E_1 & 0 \\ (1-d_f)(1-d_m)\nu_{12}E_2 & (1-d_m)E_2 & 0 \\ 0 & 0 & \alpha(1-d_s)G_{12} \end{bmatrix} \cdot [\varepsilon] \qquad (2)$$

Where

$d_f$ and $d_m$ represent tension or compression mode, depending on $\sigma_{11}$ sign,

$$d_s = 1 - \left(1-d_f^t\right)\left(1-d_f^c\right)\left(1-d_m^t\right)\left(1-d_m^c\right)$$

$$\alpha = 1 - (1-d_f)(1-d_m)\nu_{21}\nu_{12}$$

To represent the pseudo plastic behaviour of 45° plies, an elastic-plastic bilinear law is used for shear stress. Damage law is the same as for 0° and 90° plies, applied when Hashin criterion is reached.

Mechanical characteristics of the ply given in table 1 (except $G_{FC}$ and $G_{FT}$) come from characterisation tests.

## Delamination law

Delamination is represented thanks to cohesive elements, with the following behaviour law:

$$\begin{bmatrix} t_n \\ t_s \\ t_t \end{bmatrix} = \frac{1-D}{T_0} \begin{bmatrix} K_{nn} & 0 & 0 \\ 0 & K_{ss} & 0 \\ 0 & 0 & K_{tt} \end{bmatrix} \cdot \begin{bmatrix} \delta_n \\ \delta_s \\ \delta_t \end{bmatrix} \qquad (3)$$

Where ($t_n$, $t_s$, $t_t$) are stresses in the direction 3, 1 and 2, [K] is the rigidity matrix, ($\delta_n$, $\delta_s$, $\delta_t$) are separations in the direction 3, 1 and 2, $T_0$ is the initial thickness of the element, and D is the damage variable.

Damage initiates when one of the three stresses reaches its maximal value. Maximal values are the rupture values calculated from characterisation tests of composite ply: $t_n^0 = \sigma_{33} = 75$ MPa in tension, and $t_s^0 = t_t^0 = \sigma_{13} = \sigma_{23} = 150$ MPa in shear.

Propagation of damage is ruled by a bilinear softening law. The linear decrease is calculated so that energy absorbed is equal to the energy release rate at interface in each mode. Coupling between the three modes is chosen linear:

$$\sum \frac{G_i}{G_{ic}} = 1 \qquad (4)$$

After total rupture of the interfaces, contact with friction is defined between adjacent plies.

Table 1: Mechanical characteristics of T700/M21 for simulation

| | | | | |
|---|---|---|---|---|
| $E_1$ (GPa) | $E_2$ (GPa) | $G_{12}$ (GPa) | $\upsilon_{12}$ | |
| 125 | 9 | 5 | 0,4 | |
| $X^T$ (MPa) | $X^C$ (MPa) | $Y^T$ (MPa) | $Y^C$ (MPa) | $S_c$ (MPa) |
| 1950 | 1950 | 75 | 220 | 150 |
| $G_{FT}$ (mJ/mm²) | $G_{FC}$ (mJ/mm²) | $G_I$ (mJ/mm²) | $G_{II}$ (mJ/mm²) | |
| 133 | 80 | 0,35 | 1,2 | |

**Experimental / numerical comparison**

Simulation gives results close to experimental data. Figure 7 shows that curves from experiment and simulation are very similar, which means that the main phenomena are well represented: a first little peak load when the plate reaches the metallic blade, followed by a light increase of load when the two separated parts of the plate slide on the blade, then the high increase of load when they reaches the metallic base plate, and finally, the decrease of load and plateau when splaying is stabilised.

The maximum load reached during the peak (50 kN) is inferior in the simulation (35 kN), but due to the experimental dynamics effects of both the structure and the sensor (which are not completely modelled) and to the simplified rules of delamination initiation, it is to compare test and simulation. The weak value of the plateau is coherent with a crush in splaying mode, where there is low damage in plies.

Vibrations observed on the test curve, after the two peaks, are not simulated because the whole structure (steel cylinder, sensor, falling mass) is not modelled, and therefore not excited by the peak load. These vibrations do not correspond to a damage mode of the plate.

Pictures from high speed videos and simulation, in figure 8 also show a good correlation in terms of global displacement and global behaviour.

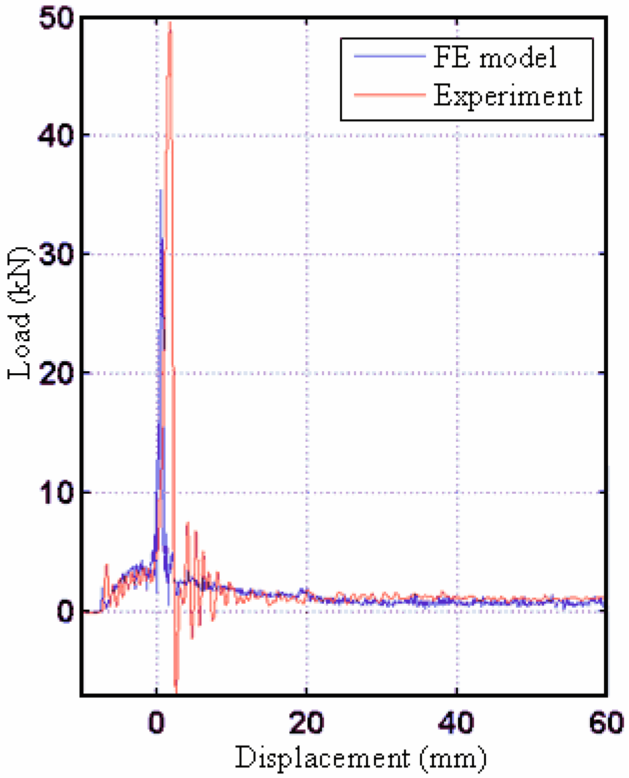


Figure 7: Comparison between experiment and simulation: Load-Displacement curve

**Analysis of energy dissipation**

The analyse of energy absorption in the crushing plateau, from simulation results, shows that in the case of splaying crush mode, in the plateau, most of the energy is dissipated in interfaces delamination. In this test configuration, it represents 60%, and only 15% for friction, and 15% for damage in plies.

**Study of influence**

Different parameters were changed to make a study of influence.

Change in friction coefficient between composite and metallic parts of the setup, from 0 to 0.3, shows that increase of friction leads to a change in front geometry (decrease of the curvature radius) and an increase of crush load and crush energy absorption. There is very small effect of composite/composite friction coefficient, varying from 0 to 0.4, as the contact surface and relative movement between plies are small during the plateau.

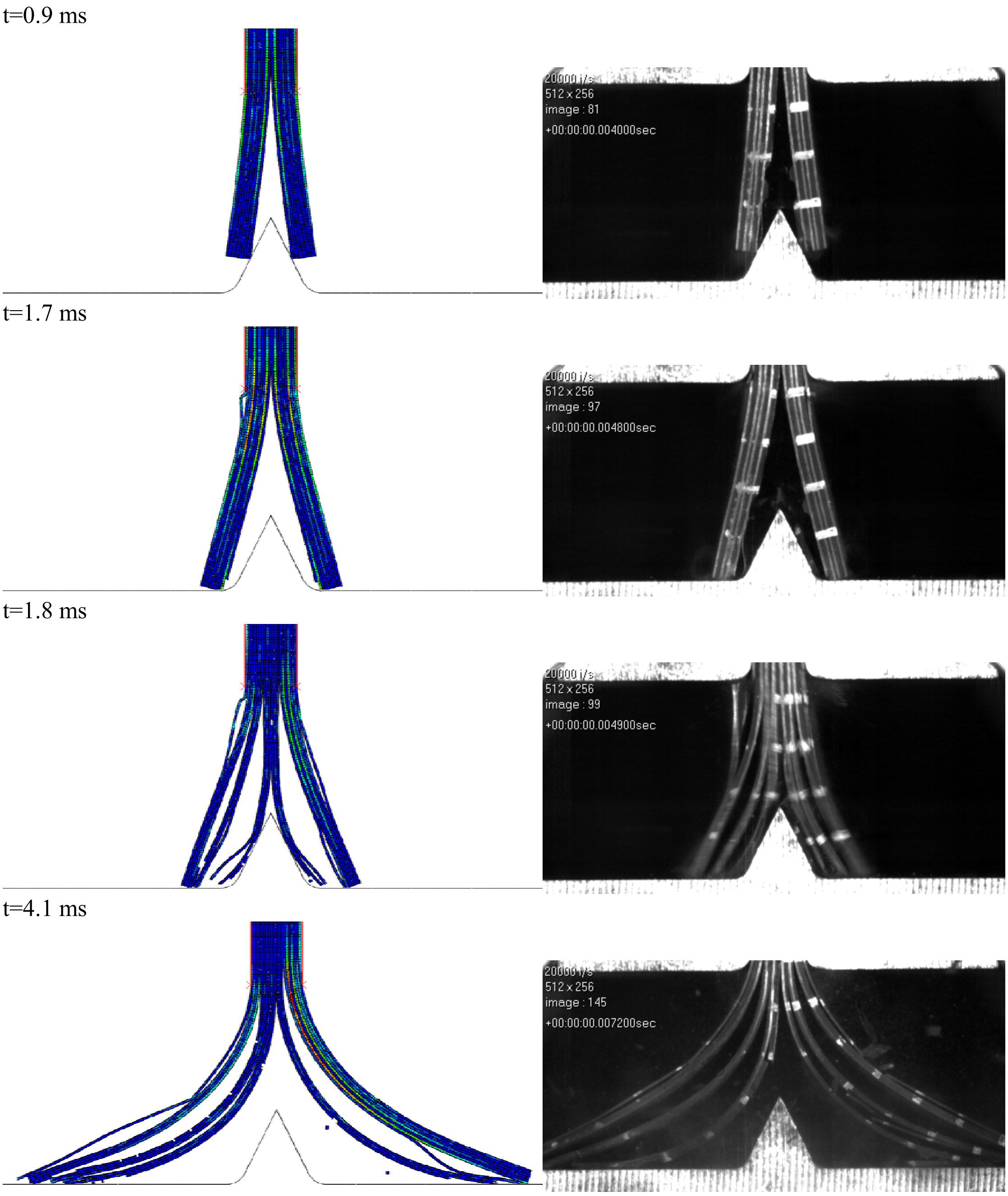


Figure 8: Comparison between experiment and simulation: visualisation of splaying

The influence of interface parameters is more complex. The increase of interface toughness by the mean of initiation stresses and critical energy release rate leads to different changes of rupture mode: decrease of the number of delaminated interface (other splaying mode, with smaller energy absorption at this step), and then increase of stresses in the plies, which lead to ruptures of plies (towards fractured splaying or fragmentation mode, with bigger energy absorption). This study of influence shows the important sensitivity of the structure behaviour under crush load to the material characteristics.

## CONCLUSION

The aim of this study was to propose a model for splaying mode in plates subjected to crush load, only dependant on the elementary material characteristics of the laminate. Thanks to precise experimental measures and observations, it is shown that simulation of crush splaying mode is possible with reasonably correct results, and that this model also enables to predict the influence of material mechanical characteristics on the behaviour of laminated plates under crush load.

However, it is clear that splaying mode is not the crush mode that absorbs the maximum of energy, and even if experiments show that in most of crush mode, outer plies are in splaying mode and help to stabilise the crush front, it is necessary to focus on simulation of fragmentation, which is the more efficient mode in terms of energy absorption.

### References


1. Hull D. "A unified approach to progressive crushing of fibre-reinforced composite tubes", *Composites science and technology* 1991;40:377-421.
2. Mamalis A.G., Robinson M., Manolakos D.E., Demosthenous G.A., Ioannidis M.B., Carruthers J. "Crashworthy capability of composite material structures", *Composite structures* 1997; 37:109-134.
3. Feraboli P., Deleo F., Garattoni F., "Efforts in the standardization of composite materials crashworthiness energy absorption", *22nd American Society for Composites Technical Conference*, Seattle, USA, September 2007.
4. McGregor C.J., Vaziri R., Poursartip A., Xiao X., "Simulation of progressive damage development in braided composite tubes under axial compression", *Composites: Part A* 2007; 11:2247-2259
5. Bisagni C., Di Pietro G., Fraschini L., Terletti D., "Progressive crushing of fiber-reinforced composite structutural components of a formula One racing car, *Composite Structures* 2005;68:491-503
6. Fleming D.C. "Finite element simulation of delamination with application to crashworthy design", *AHS 62nd annual forum*, Phoenix, USA, May 2006.
7. Pinho S.T., Camanho P.P., de Moura M.F., "Numerical simulation of the crushing process of composite materials", *Int J Crash* 2004;9(3):263-276
8. Guillon D., Rivallant S., Barrau JJ., Petiot C., Thevenet P., Pechnick N. : "Initiation and propagation mechanisms of progressive crushing in carbon-epoxy laminated plates". *ECCM13*, Stockholm, Sweden, June 2008.
9. Lavoie J.A., Kellas S. "Dynamic crush tests of energy absorbing laminated composites plates", *Composites: Part A* 1996;27:467-475.
10. Daniel L., Hogg P.J., Curtis P.T. "The crush behaviour of carbon fibre angle-ply reinforcement and the effect of interlaminar shear strength on energy absorption capability" *Composites: Part B* 2000;31:435-440.
11. Pinho S.T., Robinson P., Iannucci L., "Fracture toughness of the tensile and compressive fibre failure modes", *Composites science and technology* 2006;66:2069-2079